



10th World Conference on Neutron Radiography 5-10 October 2014

Measuring hydrogen distributions in iron and steel using neutrons

A. Griesche^{a,*}, E. Dabah^a, T. Kannengiesser^a, A. Hilger^b, N. Kardjilov^b, I. Manke^b, B. Schillinger^c

^aBAM Federal Institute for Materials Research and Testing, Unter den Eichen 87, 12205 Berlin, Germany

^bHelmholtz-Zentrum Berlin (HZB), Hahn-Meitner-Platz 1, 14109 Berlin, Germany

^cTechnische Universität München, Heinz Maier-Leibnitz Zentrum and Fakultät für Physik E21, Lichtenbergstr. 1, 85747 Garching, Germany

Abstract

Neutron tomography has been applied to investigate the mechanism of hydrogen assisted cracking in technical iron and supermartensitic steel. Rectangular technical iron block samples showed blistering due to intense hydrogen charging and the tomographic method revealed *in situ* the spatial distribution of hydrogen and cracks. Hydrogen accumulated in a small region around cracks and the cracks are filled with hydrogen gas. Cracks close to the surface contained no hydrogen. Hydrogenous tensile test samples of supermartensitic steel were pulled until rupture and showed hydrogen accumulations at the notch base and in the plastically deformed region around the fracture surface.

© 2015 The Authors. Published by Elsevier B.V. This is an open access article under the CC BY-NC-ND license (<http://creativecommons.org/licenses/by-nc-nd/4.0/>).

Selection and peer-review under responsibility of Paul Scherrer Institut

Keywords: hydrogen distribution; neutron tomography; steel

1. Introduction

Once introduced into metallic materials, hydrogen can cause a serious degradation of the mechanical properties as described e.g. by Herlach (2000). This degradation of the mechanical properties can result in a catastrophic failure of components showing a more or less brittle fracture behavior, see Lynch (2012) for a review. Since hydrogen is not solely contributing to the cracking process, this phenomenon is commonly called Hydrogen Assisted Cracking (HAC). The mechanisms of HAC are not yet completely understood and since the 1940ies

* Corresponding author. Tel.: +49-30-8104-3990; fax: +49-30-8104-3027.

E-mail address: axel.griesche@bam.de

numerous theories were suggested. However, relevant for these theories and for HAC in general is a decent knowledge about the hydrogen diffusion and trapping behavior in the respective investigated microstructure as already described by Oriani (1970). The effect of local stress and strain on the hydrogen diffusion is a topic of special interest related to the mechanical properties and fracture toughness of modern steels. First, the hydrogen dissolves interstitially in the lattice and will accumulate at sites of increased hydrostatic tensile stress due to the elastic dilatation of the lattice. Further, hydrogen also accumulates at trapping sites caused by local plastic deformation as found by Olden et al. (2008). These phenomena result from a driving force causing long-range hydrogen diffusion. These effects have been found in several experimental investigations, e.g. by Sinning (2004) using mechanical spectroscopy. From literature no experiments with bulk samples are known, which directly visualized and measured hydrogen accumulations in plastically deformed regions.

The strong interaction of neutrons with hydrogen, which is reflected by a large cross section for interaction (at a certain kinetic energy), allows achieving a sufficiently good image contrast between hydrogen enriched regions and regions which are depleted of hydrogen. The cross section for interaction of thermal neutrons with hydrogen is 82.02 barn, which is significantly larger than the interaction cross section of neutrons with iron (11.62 barn). The non-destructive property of the neutron radiography method allows here for *in situ* measurements of the hydrogen mass transport using the temporal resolution of the two-dimensional radiographic imaging or for the visualization of three-dimensional spatial hydrogen distributions using neutron tomography, which cannot be performed with conventional methods requiring prepared samples and a post mortem analysis (see e.g. Gondek et al. (2011)).

In this journal contribution, we present results from neutron tomography experiments only and refer to Beyer et al. (2011) and Dabah et al. (2014) for the results of neutron radiography measurements that we mainly used as a method for determining diffusion coefficients of hydrogen in different steel sorts and at different temperatures.

2. Experimental details

Two materials were tested with respect to their HAC behavior. First we used technical iron (ARMCOTM), which consists mainly of pure iron. Small coupons with the dimensions 45 mm height, 10 mm width and 5 mm thickness were machined from a rolled plate. The hydrogen was introduced electrochemically with a procedure described by Beyer et al. (2011). So called blistering appeared already during the charging process (see Fig. 3) indicating the occurrence of HAC. Adjacent storage in liquid nitrogen prevented any loss of hydrogen from the sample during transport to the tomography set-up. The parameters for the tomography are given in Table 1 (see also Kardjilov et al. (2011) and Williams et al. (2012)).

Table 1. Parameters used for neutron tomography at CONRAD / BER II.

Neutron flux	$2 \times 10^8 \text{ cm}^{-2} \text{ s}^{-1}$
CCD camera	Andor DW436N-BV, 16-bit, 2048x2048 pixel ²
Scintillator	10 μm Gd ₂ O ₂ S
Effective pixel size	6.4 μm
Distance sample-detector	40 mm
Aperture L/D	500
Number of projections	600
Exposure time	80 s
Spatial resolution in reconstruction	20-30 μm

The reconstruction of a set of radiographic projections yields a 3-D model of the sample. Slices taken out of the model are smoothed in the three dimensions by a 5 x 5 x 5 median filter to reduce noise that is generated by the reconstruction algorithm. The results are presented in chapter 3.1.

Second we used supermartensitic steel, a low carbon 13 % Cr martensitic stainless steel (material grade 1.1365). Bone shaped tensile samples with a rectangular cross section of 10 mm height x 5 mm thickness (6 mm x 5 mm at the notch) were produced and electrochemically charged with hydrogen, analogous to the iron samples described above. The aim of the experiment was to foster long-range hydrogen diffusion towards a sample region where plastic deformation took place with parallel recording of the hydrogen mass flux. In order to observe the diffusional mass flux we took radiographs for an hour (not presented here), while the sample was exposed to a constant tensile

load with subsequent rupture of the sample. This investigation targeted on the prerequisites necessary to initiate HAC. The sample was processed in a self-made hydraulic tensile rig (see Fig. 1) mounted in front of the detector. The mechanical load curve applied to the tensile test sample is shown in Fig. 2. The ruptured sample was rearranged for tomography and after reconstruction the tomographic data set was binned $3 \times 3 \times 3$ and median filtered $3 \times 3 \times 3$ in order to reduce noise. The results are presented in chapter 3.2.

Table 2. Parameters used for neutron radiography at ANTARES / FRM II.

Neutron flux	$2 \times 10^7 \text{ cm}^{-2} \text{ s}^{-1}$
CCD camera	IKON DZ 936-BV, 16-bit, 2048x2048 pixel ²
Scintillator	Cu and Ag doped ⁶ LiFZnS
Effective pixel size	75 μm
Distance sample-detector	40 mm
Aperture L/D	500
Exposure time	10 s

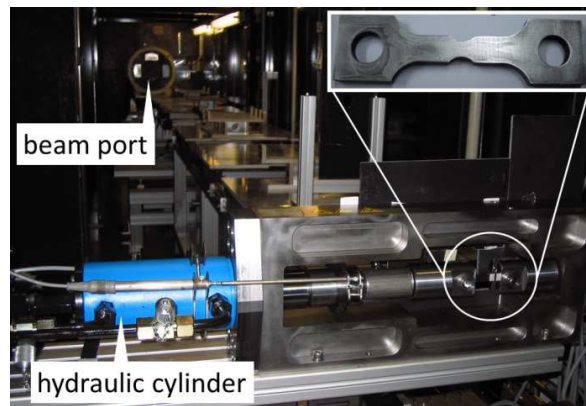


Fig. 1. Picture of the tensile rig mounted at the CONRAD experimental station. The direction of view is towards the cold neutron source. The insert shows a typical tensile test sample.

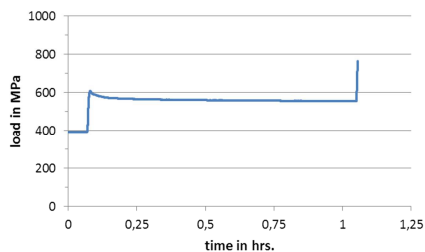


Fig. 2. Load profile of a tensile test with supermartensitic steel at room temperature. Neutron radiographs were recorded all the time with an exposure time of 10 s. The elasticity limit of non-hydrogenous supermartensitic steel is 600 MPa. Data on mechanical properties for hydrogenated material are not available in literature. The sample ruptured before the theoretical tensile strength of non-hydrogenous material of 900 MPa has been reached.

3. Results and discussion

3.1. Blistering in ARMCO

HAC already occurred during the charging of samples visible as blisters on the surface. Fig. 3 shows a metallographic specimen with blister.

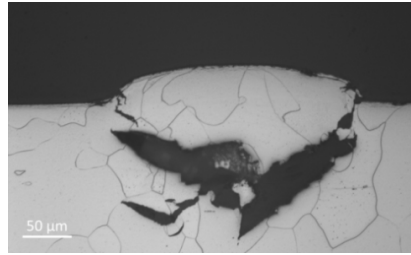


Fig. 3. Light microscopic image of a cross sectional cut of a blister in technical iron.

Obviously, the amount of hydrogen introduced in the sample exceeds the effective thermodynamic solubility close to the surface before the hydrogen is distributed in the sample's volume amongst others due to the limited diffusion velocity. Thus, the recombination of hydrogen at inner surfaces in the microstructure took place and hydrogen gas was produced. When the gas pressure exceeded the solidness of the already degraded material, cracks originated and propagated parallel to the surface sometimes lifting-up the material visible as a blister on the surface.

The use of neutron imaging gave a new insight in such degradation phenomena with subsequent cracking and blistering. We investigated blistered samples by using white beam neutron tomography and Fig. 4 shows a view into a blister (Griesche et al. (2014)). Fig. 5 presents a series of slices of the whole sample taken from the reconstructed model.

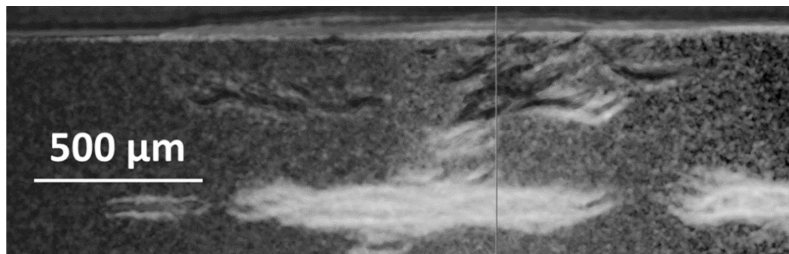


Fig. 4. Slice of a reconstructed model from a neutron tomography of a blister in an iron sample. The white color indicates the presence of hydrogen. Some cracks are filled with hydrogen gas whereas others that are located closer to the blister at the surface are not.

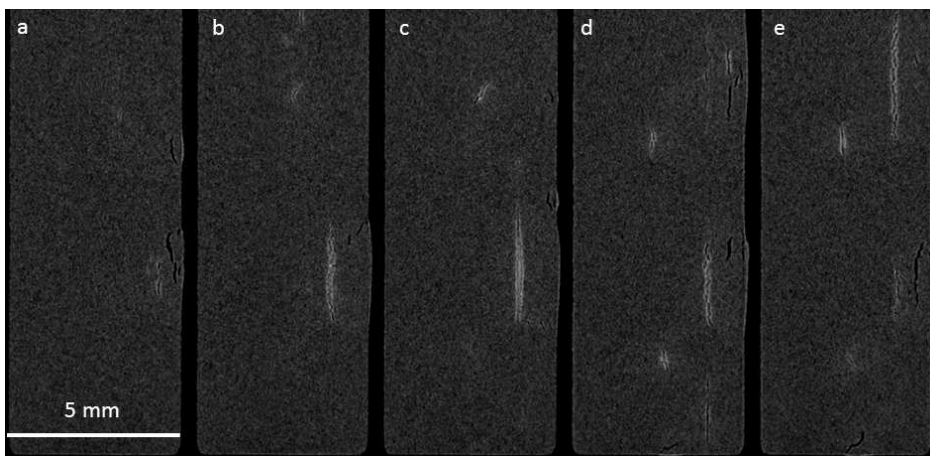


Fig. 5. Slices taken from the reconstructed model of a neutron tomography of a hydrogen-charged and blistered iron sample. The distance between each slice (a)-(e) is approx. 250 μm . The white color indicates the presence of hydrogen. Some cracks are filled with hydrogen gas whereas others that are located closer to the surface are not. The cracking direction correlates with the rolling direction.

The 3-D model allows for a detailed analysis of both the crack and hydrogen distribution. For the first time it was possible to detect and visualize hydrogen accumulations around cracks and hydrogen gas inside cracks. Also for the first time the local hydrogen content could be determined by Griesche et al. (2014). The hydrogen accumulated to 100-200 wt.ppm in a small region of $\sim 50 \mu\text{m}$ around the cracks. The concentration of the hydrogen gas in the crack's volume corresponds to a pressure of 5-15 MPa, which is an order of magnitude smaller than the yield strength of non-hydrogenous rolled iron. For more details regarding the quantification procedure of the intensity distribution in tomograms, we refer to the contribution of Kardjilov et al. in this issue of Physics Procedia. Finally, Fig. 6 gives a nice view on both the rendered surface of the reconstructed 3-D model and the interior of the sample.

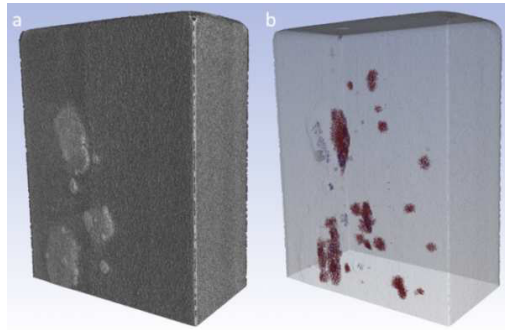


Fig. 6. Inclined view on the reconstructed 3-D model of a hydrogen charged iron sample. The rendered surface with blisters is shown in (a). Both the cracks (blue) and hydrogen (red) distribution are shown in (b). Most of the cracks are filled with hydrogen except some of the cracks closer to the surface. The latter cracks are mostly located underneath blister.

3.2. Tensile experiments with supermartensitic steel

The tensile sample ruptured at a load of $2/3$ of the theoretical tensile strength value for non-hydrogenous material. This indicates that a degradation of the mechanical material property had happened. The fractured surface, presented in Fig. 7a in form of the rendered surface of the 3-D model, shows the typical topology of HAC. A brittle outer fracture surface surrounds a honeycomb-like inner fracture surface of plastically deformed material. Interestingly, the observed hydrogen distribution shown in Fig. 7b corresponds to the regions in the sample where increased stress appeared. These regions were the surface of the notch base and the heavily plastically deformed inner part of the sample. This preliminary analysis does not allow for a full reconstruction of the history of hydrogen diffusion and HAC. Nevertheless, for the first time the crack topology and hydrogen distributions have been visualized *in situ* together in one sample. The analysis of the radiographic image series before rupture of the sample will give more insight in the chronological sequence of all steps of HAC.

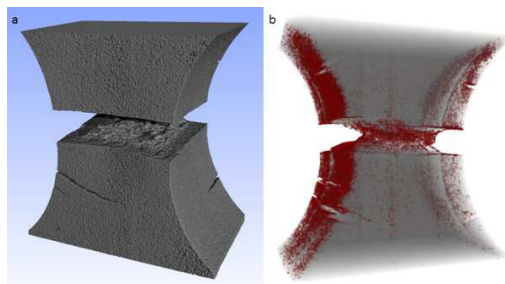


Fig. 7. Inclined view on the reconstructed 3-D model of a part of a hydrogen-charged supermartensitic tensile sample. The rendered surface of the notched area is shown in (a). The hydrogen distribution (red) is shown in (b).

4. Conclusions

We investigated hydrogen-assisted cracking and blistering in electrochemically hydrogen-charged technical iron and hydrogen-assisted cracking in electrochemically hydrogen-charged supermartensitic steel by means of neutron tomography. The main conclusions are as follows:

- Hydrogen-assisted cracking and blistering occurred during hydrogen charging in technical iron.
- In technical iron cracks having no connection to the sample's surface contained hydrogen gas. The gas pressure is at maximum 20% of the yield strength of non-hydrogenous iron. The cracks had hydrogen accumulated in small region around the cracks.
- Hydrogen accumulated at the iron sample's surface with a higher concentration at surfaces on top of blisters.
- Hydrogen accumulated at the notch base of a supermartensitic steel tensile test sample and in the region of high plastic deformation around the fracture surface.

Acknowledgements

The authors acknowledge technical support by Andreas Hannemann.

References

- Beyer, K., Kannengiesser, T., Griesche, A., Schillinger, B., 2011. Neutron radiography study of hydrogen desorption in technical iron. *Journal of Materials Science* 46, 5171-5175.
- Beyer, K., Kannengiesser, T., Griesche, A., Schillinger, B., 2011. Study of hydrogen effusion in austenitic stainless steel by time-resolved *in situ* measurements using neutron radiography. *Nuclear Instruments & Methods in Physics Research Section A - Accelerators Spectrometers Detectors and Associated Equipment* 651, 211-215.
- Dabah, E., Griesche, A., Beyer, K., Solórzano, E., Kannengiesser, T., 2014. *In situ* measurements of hydrogen diffusion in duplex stainless steels by neutron radiography, in "In situ Studies with Photons, Neutrons and Electrons Scattering II". In: Kannengiesser, T., Babu, S., Komizo, Y., Ramirez, A. (Eds.). Springer, Heidelberg, pp. 155.
- Gondek, L., Selvaraj, N., Czub, J., Figiel, H., Chapelle, D., Kardjilov, N., Hilger, A., Manke, I., 2011. Imaging of an operating LaNi_{4.8}Al_{0.2}-based hydrogen storage container, *International Journal of Hydrogen Energy* 36, 9751-9757.
- Griesche, A., Dabah, E., Kardjilov, N., Hilger, A., Manke, I., Kannengiesser, T., 2014. Imaging of hydrogen in steels using neutrons. *International Journal of Materials Research* 105, 640-644.
- Griesche, A., Dabah, E., Kardjilov, N., Hilger, A., Manke, I., Kannengiesser, T., 2014. Three-dimensional imaging of hydrogen blister in iron with neutron tomography. *Acta Materialia* 78, 14-22.
- Herlach, D., 2000. Hydrogen embrittlement of metals. *Physica B: Condensed Matter* 289-290, 443.
- Kardjilov, N., Hilger, A., Manke, I., Strobl, M., Dawson, M., Williams, S., Banhart, J., 2011. Neutron tomography instrument CONRAD at HZB. *Nuclear Instruments and Methods in Physics Research Section A: Accelerators, Spectrometers, Detectors and Associated Equipment* 651, 47-52.
- Kardjilov, N., Hilger, A., Manke, I., Griesche, A., Banhart, J., 2015. Imaging with Cold Neutrons at CONRAD-2 Facility, *Physics Procedia*, submitted.
- Lynch, S., 2012. Hydrogen embrittlement phenomena and mechanisms. *Corrosion Reviews* 30, 105-123.
- Oriani, R., 1970. Diffusion and Trapping of Hydrogen in Steel. *Acta Metallurgica* 18, 147-157.
- Olden, V., Thaulow, C., Johnsen, R., 2008. Modelling of hydrogen diffusion and hydrogen induced cracking in supermartensitic and duplex stainless steels. *Materials & Design* 29, 1934-1948.
- Sinning, H., 2004. The intercrystalline Gorsky effect. *Materials Science and Engineering A* 370, 109-113.
- Williams, S., Hilger, A., Kardjilov, N., Manke, I., Strobl, M., Douissard, P., Martin, T., Riesemeier, H., Banhart, J., 2012. Detection system for microimaging with neutrons. *Journal of Instrumentation* 7, 02014.